Sergei M. Kopeikin (Ed.)

Frontiers in Relativistic Celestial Mechanics

De Gruyter Studies in Mathematical Physics

Volume 21

Frontiers in Relativistic Celestial Mechanics

Volume 1: Theory

Edited by
Sergei M. Kopeikin

DE GRUYTER

Physics and Astronomy Classification Scheme 2010
04.20.-q, 04.25.-g, 04.25.Nx, 95.10.Ce, 95.30.Sf, 98.80.Jk

Editor
Prof. Dr. Sergei M. Kopeikin
University of Missouri
Department of Physics & Astronomy
223 Physics Bldg.
Columbia, MO 65211
USA
E-mail: kopeikins@missouri.edu

ISBN 978-3-11-033747-1
e-ISBN 978-3-11-033749-5
Set-ISBN 978-3-11-035932-9
ISSN 2194-3532

Library of Congress Cataloging-in-Publication Data
A CIP catalog record for this book has been applied for at the Library of Congress.

Bibliographic information published by the Deutsche Nationalbibliothek
The Deutsche Nationalbibliothek lists this publication in the Deutsche Nationalbibliografie; detailed bibliographic data are available in the Internet at http://dnb.dnb.de.

Typesetting: le-tex publishing services GmbH, Leipzig
Printing and binding: CPI books GmbH, Leck
♾ Printed on acid-free paper
Printed in Germany

www.degruyter.com

This Festschrift is dedicated to Professor *Victor A. Brumberg*,
for his enthusiasm and devotion to the science of relativistic celestial mechanics,
and to celebrate his 80th birthday.

List of contributors

Prof. Dr. Thibault Damour
Institute of Advanced Scientific Studies (IHÉS)
35 route de Chartres
Bures sur Yvette, F-91440
France
E-mail: damour@ihes.fr

Prof. Dr. Toshifumi Futamase
Tohoku University
Astronomical Institute
Sendai 980-8578
Japan
E-mail: tof@astr.tohoku.ac.jp

Prof. Dr. Sergei Kopeikin
University of Missouri
Department of Physics & Astronomy
223 Physics Bldg.
Columbia, MO 65211
USA
E-mail: kopeikins@missouri.edu

Prof. Dr. Gerhard Schäfer
Friedrich Schiller University Jena
Institute of Theoretical Physics
Max-Wien-Platz 1
D-07743 Jena
Germany
E-mail: gos@tpi.uni-jena.de

Prof. Dr. Michael Soffel
Dresden University of Technology
Lohrmann Observatory TU Dresden
Planetary Geodesy
Mommsenstr 13
01062 Dresden
Germany
E-mail: soffel@rcs.urz.tu-dresden.de

Dr. Pavel Korobkov
Solovetsky Monastery
Arkhangelsk Region 164070
Russia

Dr. Alexander Petrov
Moscow Lomonosov State University
Sternberg Astronomical Institute
Universitetskiy Prospect 13
Moscow 119992
Russia
E-mail: alex.petrov55@gmail.com

Dr. Xie Yi
Nanjing University
Department of Astronomy
22 Hankou Road
Nanjing Jiangsu 210093
P. R. China
E-mail: yixie@nju.edu.cn

Contents

List of figures

Preface

The science of relativistic celestial mechanics is an essential branch of the modern gravitational physics, a branch exploring the fundamental structure of spacetime by studying motion of massive bodies such as black holes, stars, planets, as well as elementary particles, including photons, in gravitational field. It establishes basic theoretical principles for calculation and interpretation of various relativistic effects and phenomena observed in astrophysical stellar systems and in the solar system. Relativistic celestial mechanics of massless particles like photons is more known among astronomers as relativistic astrometry. An indefeasible branch of gravitational physics, it is required to map the coordinate description of motion of celestial bodies into parameter space of observables. Theoretical progress in understanding the orbital motion of celestial bodies would be inconceivable without a corresponding improvement in mathematical description of motion of light rays in stationary and time-dependent gravitational field.

Relativistic celestial mechanics has received a special attention in the gravitational-wave astronomy. Being on its way to direct detection of gravitational waves emitted by coalescing binary stars, the gravitational-wave astronomy urgently needs highly precise templates of gravitational waves emitted by the stars at the very last stage of their orbital motion, just a few seconds before the stars collide and a catastrophic supernova explosion takes place. Therefore, development of theoretical tools of relativistic celestial mechanics has a fundamental significance for achieving further progress in gravitational-wave astronomy which is expected to become a primary experimental tool bringing much deeper understanding of the nature of gravitational field and the underlying geometric structure of the spacetime manifold.

Relativistic celestial mechanics was a subject of active research by many notable scientists, including A. Einstein, H. Lorentz, V. A. Fock, T. Levi-Civita, L. Infeld, S. Chandrasekhar, J. Ehlers, G. C. McVittie, and others who elaborated on various approaches to the equations of motion of celestial bodies and the theory of astronomical observations in general relativity. More recently, a valuable contribution to relativistic celestial mechanics was made by T. Damour, G. Schäfer, M. Soffel, C. M. Will, K. Nordtvedt, T. Futamase, K. S. Thorne, W. G. Dixon, L. Blanchet, and I. Rothstein. A key figure of relativistic celestial mechanics of the second half of twentieth century has been Victor A. Brumberg, a scholar who presently lives in Boston (USA) and who is still active in research. Victor A. Brumberg has made a significant contribution to general relativity and the science of relativistic planetary ephemerides of the solar system. He mentored and inspired many researchers around the globe (including the Editor of this book) to start working in the field of relativistic celestial mechanics. The very term "relativistic celestial mechanics" was introduced by Victor. A. Brumberg in his famous monograph "Relativistic Celestial Mechanics" published in 1972 by Nauka (Science) – the main scientific publisher of the USSR – in Moscow. For the next two decades this monograph remained the most authoritative reference and the source of invaluable information for researchers working on relativistic equations of motion and experimental testing of general relativity. Victor A. Brumberg received the 2008 Brower Award from the Division of Dynamic Astronomy of the American Astronomical Society. The Brouwer Award was established to recognize outstanding contributions to the field of dynamical astronomy, including celestial mechanics, astrometry, geophysics, stellar systems, galactic, and extragalactic dynamics.

This book is a first volume of Festschrift aimed to honor the scientific influence and achievements of V. A. Brumberg, and to celebrate his 80th birthday which took place on February 12, 2013. The book appears on the eve of another remarkable date – 100 years of Einstein's general relativity – the theory which dramatically changed the world of theoretical physics by opening new fascinating opportunities in the scientific study of fundamental laws of Nature. The volume consists of seven chapters discussing the recent theoretical advances in relativistic celestial mechanics and related areas of theoretical physics and astronomy.

Chapter 1, written by T. Damour, introduces the amazingly rich mathematics of the relativistic two-body problem. Solution of this problem within the Newtonian mechanics is cornerstone material that can be found in any textbook on celestial mechanics. On the other hand, complete solution of this problem within general relativity has not been yet obtained, even though it has been subject of numerous analytical investigations. The root of the difficulty is lying in the nonlinear character of gravitational interaction in Einstein's theory of gravity, which prevents us from finding an exact solution to the problem. Hence, the analytic solution can be ascertained only by making use of successive approximations. The method includes complicated, often diverging integrals which require development of regularization technique based on the theory of distributions. Additional difficulties arise due to the emission of gravitational waves by the two-body system, an effect generating a back reaction on the motion of the bodies – the so-called radiation-reaction force. After reviewing some of the methods used to tackle these problems, Chapter 1 focuses on a new, recently introduced approach to the motion and radiation of (comparable-mass) binary systems: the effective-onebody (EOB) formalism. The basic elements of this formalism are reviewed, and some of its recent developments are discussed. Several recent tests of EOB predictions against numerical simulations have shown the aptitude of the EOB formalism to provide accurate description of the dynamics and radiation of various binary systems (comprising black holes or neutron stars) in regimes that are inaccessible to other analytical approaches such as the last orbits and the merger of comparable mass black holes. Chapter 1 provides weighty arguments that, in synergy with numerical simulations, the post-Newtonian theory and gravitational self-force (GSF) computations, the EOB formalism is likely to provide an efficient way of accurately computing the numerous template waveforms that are needed for the purposes of gravitational wave data analysis.

Chapter 2, written by G. Schäfer, continues theoretical analysis of the two-body problem in general relativity, by making use of the advanced Hamiltonian technique introduced by Arnovitt, Deser, and Misner (ADM formalism). The Hamiltonian setting of general relativity allows a very elegant and transparent treatment of the dynamics and motion of gravitating systems. Crucial in that context is the computation of the reduced Hamiltonian which generates the dynamics of both the gravitating objects and the gravitational field. Based on the framework of post-Newtonian approximation, Chapter 2 covers the dynamics and motion of spinning compact binaries up to the fourth post-Newtonian approximation.

Chapter 3, written by Y. Xie and S. Kopeikin, presents a covariant theory of post-Newtonian equations of translational motion of extended bodies in an N-body system. It significantly extends the results obtained in 1970–80th by W. G. Dixon. The new theory is based on the combined BK-DSX theory extended to the realm of the scalar-tensor theory of gravity. It introduces one more type of multipole moments to the formalism – the scalar-type moments. The chapter explains how to build the local and global coordinates in a system of N extended bodies, and offers a procedure intended to derive the translational equations of motion of the bodies, including all internal multipoles. It is proven that any integral moment, which depends on the internal structure of the bodies in a way different from the “canonical” Blanchet–Damour moments, vanishes from the translational equations of motion. Finally, a covariant form of the post-Newtonian equations of motion of extended bodies, with all internal multipoles taken into account, is derived by applying a technique proposed by Thorne and Hartle in 1985. The translational equations of motion derived in this way represent a profound generalization of the Mathisson–Papapetrou–Dixon equations of motion.

Chapter 4, written by M. Soffel, furnishes an account of the Damour–Soffel–Xu (DSX) formalism of relativistic reference frames in N-body system. The DSX formalism is an extension of the formalism advanced in 1988 by Brumberg and Kopeikin (the BK formalism) to build the post-Newtonian theory of astronomical reference frames in the solar system. The BK-DSX theory is based on the complementary use of N local coordinate charts attached to each body, which are built to describe rotation and local dynamics of the body, and of a global coordinate chart, which is intended to describe the orbital motion of the bodies. The advantage of the DSX formalism, compared to the BK formalism, is in the systematic use of well-defined mass-type and spin-type multipole moments of the extended bodies. Chapter 4 explains the DSX formalism in a concise but mathematically rigorous form.

Chapter 5, written by P. Korobkov and S. Kopeikin, delivers theoretical tools for solving the problem of propagation of photons through multipolar gravitational field of an isolated astronomical system emitting gravitational waves. The solution is written in the first post-Minkowskian approximation of general relativity. The Chapter opens with an introduction to the linearized theory of retarded gravitational potentials of the Lienard–Wiechert type. The Chapter then deals with derivation of differential equations of light geodesics with retarded argument. Mathematical technique of integrating these equations is proposed, and a solution is found in a closed form. It is demonstrated that the leading-order observable relativistic effects depend on the value of the multipoles of the isolated system and their time derivatives taken at the retarded instant of time. This retardation is caused by finite speed of propagation of gravity, and for this reason the relativistic effects do not depend on the integrated values of the multipoles taken along the past world line of the isolated system. The integration technique reproduces the known results of integration of equations of light rays in the stationary approximation of a gravitational lens and in the approximation of a plane gravitational wave. Two limiting cases of small and large impact parameters of a light ray with respect to the isolated system are worked out in more detail. It is shown that in case of a small impact parameter the leading-order terms in the solution for light propagation depend neither on radiative nor on intermediate zone components of the gravitational field, but the main effect comes from the near-zone values of the multipole moments. This radiative-zone effacing property makes it much more difficult (but not impossible!) to directly detect gravitational waves by astronomical instruments than it was assumed by some researchers. Chapter 5 also presents analytical treatment of time-delay and light-ray bending in the case of large impact parameter corresponding to the approximation of plane gravitational wave. Explicit expressions for the time delay and the deflection angle of the light ray are obtained in terms of the transverse-traceless (TT) multipole moments of the gravitating system. This result can be directly applied to interpretation of observables in gravitational wave interferometers.

Development of the canonical theory of post-Newtonian approximations in relativistic celestial mechanics relies upon the key concept of an isolated astronomical system, under assumption that background spacetime is flat. The standard post-Newtonian theory of motion is instrumental in explanation of the existing experimental data on binary pulsars, satellite, and lunar laser ranging, and in building precise ephemerides of planets in the solar system. Recent cosmological studies indicate that the standard post-Newtonian mechanics fails to describe more subtle dynamical effects in the small-scale structure formation and in the motion of galaxy clusters comprising astronomical systems. In those settings, the curvature of the expanding universe interacts with the local gravitational field of the astronomical system and, as such, cannot be ignored. Therefore, working out theoretical foundations of relativistic celestial mechanics of isolated astronomical system residing on cosmological manifold is worthwhile. Additional motivation for this comes from the gravitational wave astronomy which will study relativistic celestial mechanics of binary systems in very distant galaxies residing at the edge of the visible universe. Dynamical evolution of the binaries on a cosmological background is primarily governed by multipolar structure of its own gravitational field, but is also intrinsically connected with the cosmological parameters of the background manifold. These parameters are determined by the content of the substance filling up the universe, whose most enigmatic components are the dark matter and dark energy. Tracking down the orbital motion of binary systems in distant galaxies at gravitational wave observatories is promising for doing precise cosmology. It is very likely that observation of binaries with gravitational wave detectors will supersede the precision of measurement of cosmological parameters by radio astronomical technique. These interesting questions are illuminated in Chapters 6 and 7 of this book.

Chapter 6, authored by T. Futamase, outlines the results of his research on the emergence of the cosmological metric in a lumpy universe, a line of study known as the averaging problem in cosmology. The Chapter also discusses the gravitational backreaction by local nonlinear inhomogeneities on the cosmic expansion, in the framework of general relativity. The problem became important after the discovery of the cosmic acceleration associated with the presence of dark energy. After a brief review of the subject, T. Futamase presents in detail his own approach to analytical calculation of the backreaction, which allows him to overview the apparent discrepancies between previous works using different approaches and gauges. Chapter 6 partially resolves these discrepancies by defining the spatially averaged energy density of matter as a conserved quantity referred to a sufficiently large volume of comoving space. It is shown that the backreaction behaves like a positive-curvature term in the averaged Friedmann–Lemître–Robertson–Walker (FLRW) universe. It neither accelerates nor decelerates the cosmic expansion in a matter-dominated universe, while the cosmological constant induces a new type of backreaction with the equation-of-state parameter being $-4/3$. However, the effective energy density remains negative, and thus it decreases the acceleration.

Chapter 7, written by A. Petrov and S. Kopeikin, extends the post-Newtonian approximation of general relativity to the realm of cosmology, by making use of a geometric theory of Lagrangian perturbations of an FLRW cosmological manifold. The Lagrangian for a perturbed cosmological model includes the dark matter, the dark energy, and the ordinary baryonic matter. The Lagrangian is decomposed in an asymptotic Taylor series around a background FLRW manifold, with the small parameter being the magnitude of the metric–tensor perturbation. Each term of the series decomposition is kept gauge invariant. The asymptotic nature of the Lagrangian decomposition does not require the post-Newtonian perturbations to be small, though computationally it works most effectively when the perturbed metric is close to the background one. The Lagrangian of dark matter is treated as an ideal fluid described by an auxiliary scalar field called the Clebsch potential. The dark energy is associated with a single scalar field of an unspecified potential energy. The scalar fields of dark matter and dark energy are taken as independent dynamical variables which play the role of generalized coordinates in the Lagrangian formalism. This allows the authors to implement the powerful methods of variational calculus, to derive gauge-invariant field equations to be used in the post-Newtonian celestial mechanics in an expanding universe. The equations generalize the field equations of the post-Newtonian theory in an asymptotically flat spacetime, by taking into account the cosmological effects without assuming a rather artificial vacuole model of an isolated system (like those proposed by Einstein and Strauss, McVittie, and Bonnor). A new cosmological gauge is proposed, which generalizes the de Donder (harmonic) gauge of the post-Newtonian theory in an asymptotically flat spacetime. The new gauge significantly simplifies the gravitational field equations and reduces them to wave equations, the latter being differential equations of Bessel's type. The new gauge also allows the authors to find out the cosmological models wherein the field equations are fully decoupled and can be solved analytically. The residual gauge freedom is explored and the residual gauge transformations are formulated in the form of wave equations for gauge functions. Chapter 7 demonstrates how cosmological effects interfere with the local distribution of matter of the isolated system and its orbital dynamics. The Chapter also offers a precise mathematical definition of the Newtonian limit for an isolated system residing on a cosmological manifold. The results of the chapter can be useful in the galactic astronomy, to study the dynamics of clusters of galaxies, and in the gravitational wave astronomy, for discussing the impact of cosmological effects on generation and propagation of gravitational waves emitted by coalescing binaries.

Over the past 30 years, relativistic celestial mechanics has experienced radical progress both in theory and in experimental testing of general relativity. The present volume cannot embrace it in its entirety. For further reading on recent developments in relativistic celestial mechanics, we recommend the following review articles and textbooks:

Asada, H., Futamase, T. and Hogan, P., "Equations of Motion in General Relativity," Oxford University Press: Oxford, 2011

Brumberg, V. A., "Celestial mechanics: past, present, future," *Solar System Research*, Vol. 47, Issue 5, pp. 347–358 (2013)

Brumberg, V. A., "Relativistic Celestial Mechanics on the verge of its 100 year anniversary" (Brouwer Award lecture), *Celestial Mechanics and Dynamical Astronomy*, Vol. 106, Issue 3, pp. 209–234 (2010)

Brumberg, V. A., "Relativistic Celestial Mechanics," *Scholarpedia*, Vol. 5, Issue 8, #10669. URL (cited on Jan 12, 2014) http://www.scholarpedia.org/article/Relativistic_Celestial_Mechanics

Brumberg, V. A., "Essential Relativistic Celestial Mechanics," Adam Hilger: Bristol, 1991

Blanchet, L., "Gravitational Radiation from Post-Newtonian Sources and Inspiralling Compact Binaries," Living Reviews in Relativity 5, 3 (2002). URL (cited on Jan. 12, 2014) http://www.livingreviews.org/lrr-2002-3

Damour, T., "The problem of motion in Newtonian and Einsteinian gravity," In: Three Hundred Years of Gravitation, Eds. Hawking, S. W. and Israel, W., Cambridge University Press: Cambridge, 1987. pp. 128–198

Goldberger, W. D. and Rothstein, I. Z., "Effective field theory of gravity for extended objects," Physical Review D, Vol. 73, Issue 10, id. 104029 (2006)

Kopeikin, S., Efroimsky, M. and G. Kaplan, "Relativistic Celestial Mechanics of the Solar System," Wiley-VCH: Berlin, 2011

Soffel, M. and Langhans, R., "Space–Time Reference Systems," Springer-Verlag: Berlin, 2013

February 12, 2014

Editor: Sergei Kopeikin
University of Missouri, USA

Thibault Damour

The general relativistic two-body problem

1 Introduction

The general relativistic problem of motion, i.e. the problem of describing the dynamics of N gravitationally interacting extended bodies, is one of the cardinal problems of Einstein's theory of gravitation. This problem has been investigated from the early days of development of general relativity, notably through the pioneering works of Einstein, Droste, and de Sitter. These authors introduced the post-Newtonian (PN) approximation method, which combines three different expansions: (i) a weak-field expansion ($g_{\mu\nu} - \eta_{\mu\nu} \equiv h_{\mu\nu} \ll 1$); (ii) a slow-motion expansion ($v/c \ll 1$); a near-zone expansion ($\frac{1}{c}\,\partial_t\, h_{\mu\nu} \ll \partial_x h_{\mu\nu}$). PN theory could be easily worked out to derive the first post-Newtonian (1PN) approximation, i.e. the leading-order general relativistic corrections to Newtonian gravity (involving one power of $1/c^2$). However, the use of the PN approximation for describing the dynamics of N extended bodies turned out to be fraught with difficulties. Most of the early derivations of the 1PN-accurate equations of motion of N bodies turned out to involve errors: this is, in particular, the case of the investigations by Droste [1], de Sitter [2], Chazy [3], and Levi-Civita [4]. These errors were linked to incorrect treatments of the internal structures of the bodies. Apart from the remarkable 1917 work of Lorentz and Droste [5] (which seems to have remained unnoticed during many years), the first correct derivations of the 1PN-accurate equations of motion date from 1938, and were obtained by Einstein et al. [6], and Eddington and Clark [7]. After these pioneering works (and the investigations they triggered, notably in Russia [8] and Poland), the general relativistic N-body problem reached a first stage of maturity and became codified in various books, notably in the books of Fock [9], Infeld and Plebanski [10], and in the second volume of the treatise of Landau and Lifshitz (starting, at least, with the 1962 second English edition).

We have started by recalling the early history of the general relativistic problem of motion both because Victor Brumberg has always shown a deep knowledge of this history, and because, as we shall discuss below, some of his research work has contributed to clarifying several of the weak points of the early PN investigations (notably those linked to the treatment of the internal structures of the N bodies).

For many years, the 1PN approximation turned out to be accurate enough for applying Einstein's theory to known N-body systems, such as the solar system, and various binary stars. It is still true today that the 1PN approximation (especially when

Thibault Damour: Institut des Hautes Études Scientifiques (IHÉS), 35 route de Chartres, F-91440, Bures sur Yvette, France

used in its multichart version, see below) is adequate for describing general relativistic effects in the solar system. However, the discovery in the 1970s of binary systems comprising strongly self-gravitating bodies (black holes or neutron stars) has obliged theorists to develop improved approaches to the N-body problem. These improved approaches are not limited (as the traditional PN method) to the case of weakly self-gravitating bodies and can be viewed as modern versions of the Einstein–Infeld–Hoffmann classic work [6].

In addition to the need of considering strongly self-gravitating bodies, the discovery of binary pulsars in the mid-1970s (starting with the Hulse–Taylor pulsar PSR 1913 + 16) obliged theorists to go beyond the 1PN ($O(v^2/c^2)$) relativistic effects in the equations of motion. More precisely, it was necessary to go to the 2.5PN approximation level, i.e. to include terms $O(v^5/c^5)$ beyond Newton in the equations of motion. This was achieved in the 1980s by several groups [11–15]. (Let us note that important progress in obtaining the N-body metric and equations of motion at the 2PN level was achieved by the Japanese school in the 1970s [16–18].)

Motivation for pushing the accuracy of the equations of motion beyond the 2.5PN level came from the prospect of detecting the gravitational wave signal emitted by inspiralling and coalescing binary systems, notably binary neutron star (BNS) and binary black hole (BBH) systems. The 3PN-level equations of motion (including terms $O(v^6/c^6)$ beyond Newton) were derived in the late 1990s and early 2000s [19–22, 80] (they have been recently rederived in [24]). Recently, the 4PN-level dynamics has been tackled in [25–28].

Separately from these purely analytical approaches to the motion and radiation of binary systems, which have been developed since the early days of Einstein's theory, numerical relativity (NR) simulations of Einstein's equations have relatively recently (2005) succeeded (after more than 30 years of developmental progress) to stably evolve binary systems made of comparable mass black holes [29–32]. This has led to an explosion of works exploring many different aspects of strong-field dynamics in general relativity, such as spin effects, recoil, relaxation of the deformed horizon formed during the coalescence of two black holes to a stationary Kerr black hole, high-velocity encounters, etc.; see [33] for a review and [34] for an impressive example of the present capability of NR codes. In addition, recently developed codes now allow one to accurately study the orbital dynamics, and the coalescence of BNSs [35]. Much physics remains to be explored in these systems, especially during and after the merger of the neutron stars (which involves a much more complex physics than the pure-gravity merger of two black holes).

Recently, a new source of information on the general relativistic two-body problem has opened: gravitational self-force (GSF) theory. This approach goes one step beyond the test-particle approximation (already used by Einstein in 1915) by taking into account self-field effects that modify the leading-order geodetic motion of a small mass m_1 moving in the background geometry generated by a large mass m_2. After some ground work (notably by DeWitt and Brehme) in the 1960s, GSF theory has recently undergone rapid developments (mixing theoretical and numerical methods) and can now yield numerical results that yield access to new information on strong-field dynamics in the extreme mass-ratio limit $m_1 \ll m_2$. See Ref. [36] for a review.

Each of the approaches to the two-body problem mentioned so far, PN theory, NR simulations, and GSF theory, has their advantages and their drawbacks. It has become recently clear that the best way to meet the challenge of accurately computing the gravitational waveforms (depending on several continuous parameters) that are needed for a successful detection and data analysis of GW signals in the upcoming LIGO/Virgo/GEO/... network of GW detectors is to combine knowledge from all the available approximation methods: PN, NR, and GSF. Several ways of doing so are a priori possible. For instance, one could try to directly combine PN-computed waveforms (approximately valid for large enough separations, say $r \gtrsim 10\,G(m_1 + m_2)/c^2$) with NR waveforms (computed with initial separations $r_0 > 10\,G(m_1 + m_2)/c^2$ and evolved up to merger and ringdown). However, this method still requires too much computational time, and is likely to lead to waveforms of rather poor accuracy, see, e.g. [37, 38].

On the other hand, 5 years before NR succeeded in simulating the late inspiral and the coalescence of BBHs, a new approach to the two-body problem was proposed: the effective one body (EOB) formalism [39–42]. The basic aim of the EOB formalism is to provide an analytical description of both the motion and the radiation of coalescing binary systems over the entire merger process, from the early inspiral, right through the plunge, merger, and final ringdown. As early as 2000 [40] this method made several quantitative and qualitative predictions concerning the dynamics of the coalescence, and the corresponding GW radiation, notably: (i) a blurred transition from inspiral to a "plunge" that is just a smooth continuation of the inspiral, (ii) a sharp transition, around the merger of the black holes, between a continued inspiral and a ring-down signal, and (iii) estimates of the radiated energy and of the spin of the final black hole. In addition, the effects of the individual spins of the black holes were investigated within the EOB [42, 43] and were shown to lead to a larger energy release for spins parallel to the orbital angular momentum, and to a dimensionless rotation parameter J/E^2 always smaller than unity at the end of the inspiral (so that a Kerr black hole can form right after the inspiral phase). All those predictions have been broadly confirmed by the results of the recent numerical simulations performed by several independent groups (for a review of numerical relativity results and references see [33]). Note that, in spite of the high computer power used in NR simulations, the calculation, checking, and processing of one sufficiently long waveform (corresponding to specific values of the many continuous parameters describing the two arbitrary masses, the initial spin vectors, and other initial data) takes on the order of 1 month. This is a very strong argument for developing analytical models of waveforms. For a recent comprehensive comparison between analytical models and numerical waveforms see [44].

In this work, we shall briefly review only a few facets of the general relativistic two-body problem (see, e.g. [45] and [46] for recent reviews dealing with other facets of, or approaches to, the general relativistic two-body problem). First, we shall recall the essential ideas of the multichart approach to the problem of motion, having especially in mind its application to the motion of compact binaries, such as BNS or BBH systems. Then we shall focus on the EOB approach to the motion and radiation of binary systems, from its conceptual framework to its comparison to NR simulations.

2 Multichart approach to the N-body problem

The traditional (text book) approach to the problem of motion of N separate bodies in GR consists of solving, by successive approximations, Einstein's field equations (we use the signature $-+++$)

$$R_{\mu\nu} - \frac{1}{2} R\, g_{\mu\nu} = \frac{8\pi G}{c^4} T_{\mu\nu} \,, \tag{2.1}$$

together with their consequence

$$\nabla_\nu T^{\mu\nu} = 0 \,. \tag{2.2}$$

To do so, one assumes some specific matter model, say a perfect fluid,

$$T^{\mu\nu} = (\varepsilon + p)\, u^\mu u^\nu + p\, g^{\mu\nu} \,. \tag{2.3}$$

One expands (say in powers of Newton's constant) the metric,

$$g_{\mu\nu}(x^\lambda) = \eta_{\mu\nu} + h^{(1)}_{\mu\nu} + h^{(2)}_{\mu\nu} + \cdots \,, \tag{2.4}$$

and use the simplifications brought by the "post-Newtonian" approximation ($\partial_0 h_{\mu\nu} = c^{-1}\partial_t h_{\mu\nu} \ll \partial_i h_{\mu\nu}$; $v/c \ll 1$, $p \ll \varepsilon$). Then one integrates the local material equation of motion (2.2) over the volume of each separate body, labelled say by $a = 1, 2, \ldots, N$. In so doing, one must define some "center of mass" z^i_a of body a, as well as some (approximately conserved) "mass" m_a of body a, together with some corresponding "spin vector" S^i_a and, possibly, higher multipole moments.

An important feature of this traditional method is to use a *unique coordinate chart* x^μ to describe the full N-body system. For instance, the center of mass, shape, and spin of each body a are all described within this common coordinate system x^μ. This use of a single chart has several inconvenient aspects, even in the case of weakly self-gravitating bodies (as in the solar system case). Indeed, it means for instance that a body which is, say, spherically symmetric in its own "rest frame" X^α will appear as deformed into some kind of ellipsoid in the common coordinate chart x^μ. Moreover, it is not clear how to construct "good definitions" of the center of mass, spin vector, and higher multipole moments of body a, when described in the common coordinate chart x^μ. In addition, as we are possibly interested in the motion of strongly self-gravitating bodies, it is not a priori justified to use a simple expansion of the type (2.4) because $h^{(1)}_{\mu\nu} \sim \sum_a Gm_a/(c^2\,|\boldsymbol{x} - \boldsymbol{z}_a|)$ will not be uniformly small in the common coordinate system x^μ. It will be small if one stays far away from each object a, but, it will become of order unity on the surface of a compact body.

These two shortcomings of the traditional "one-chart" approach to the relativistic problem of motion can be cured by using a *"multichart" approach*. The multichart approach describes the motion of N (possibly, but not necessarily, compact) bodies by using $N + 1$ separate coordinate systems: (i) one *global* coordinate chart x^μ ($\mu = 0, 1, 2, 3$) used to describe the spacetime outside N "tubes," each containing one body, and (ii) N *local* coordinate charts X^α_a ($\alpha = 0, 1, 2, 3$; $a = 1, 2, \ldots, N$) used to describe the spacetime in and around each body a. The multichart approach was first used to discuss the motion of black holes and other compact objects [47–54]. Then it was also found to be very convenient for describing, with the high-accuracy required for dealing with modern technologies such as VLBI, systems of N weakly self-gravitating bodies, such as the solar system [55, 56].

The essential idea of the multichart approach is to combine the information contained in *several expansions*. One uses both a global expansion of the type (2.4) and several local expansions of the type

$$G_{\alpha\beta}(X^\gamma_a) = G^{(0)}_{\alpha\beta}(X^\gamma_a; m_a) + H^{(1)}_{\alpha\beta}(X^\gamma_a; m_a, m_b) + \cdots\,, \tag{2.5}$$

where $G^{(0)}_{\alpha\beta}(X; m_a)$ denotes the (possibly strong-field) metric generated by an isolated body of mass m_a (possibly with the additional effect of spin).

The separate expansions (2.4) and (2.5) are then "matched" in some overlapping domain of common validity of the type $Gm_a/c^2 \lesssim R_a \ll |\boldsymbol{x} - \boldsymbol{z}_a| \ll d \sim |\boldsymbol{x}_a - \boldsymbol{x}_b|$ (with $b \neq a$), where one can relate the different coordinate systems by expansions of the form

$$x^\mu = z^\mu_a(T_a) + e^\mu_i(T_a)\,X^i_a + \tfrac{1}{2}\,f^\mu_{ij}(T_a)\,X^i_a\,X^j_a + \cdots\,. \tag{2.6}$$

The multichart approach becomes simplified if one considers *compact* bodies (of radius R_a comparable to $2\,Gm_a/c^2$). In this case, it was shown [52], by considering how the "internal expansion" (2.5) propagates into the "external" one (2.4) via the matching (2.6), that, *in general relativity*, the internal structure of each compact body was *effaced* to a very high degree, when seen in the external expansion (2.4). For instance, for nonspinning bodies, the internal structure of each body (notably the way it responds to an external tidal excitation) shows up in the external problem of motion only at the *fifth post-Newtonian* (5PN) approximation, i.e. in terms of order $(v/c)^{10}$ in the equations of motion.

This *effacement of internal structure* indicates that it should be possible to simplify the rigorous multichart approach by skeletonizing each compact body by means of some delta-function source. Mathematically, the use of distributional sources is delicate in a nonlinear theory such as GR. However, it was found that one can reproduce the results of the more rigorous matched-multichart approach by treating the divergent integrals generated by the use of delta-function sources by means of (complex) analytic continuation [52]. In particular, analytic continuation in the dimension of space d [57] is very efficient (especially at high PN orders).

Finally, the most efficient way to derive the general relativistic equations of motion of N compact bodies consists of solving the equations derived from the action (where $g \equiv -\det(g_{\mu\nu})$)

$$S = \int \frac{d^{d+1}x}{c} \sqrt{g}\, \frac{c^4}{16\pi G} R(g) - \sum_a m_a c \int \sqrt{-g_{\mu\nu}(z_a^\lambda)\, dz_a^\mu\, dz_a^\nu}\,, \tag{2.7}$$

formally using the standard weak-field expansion (2.4), but considering the space dimension d as an arbitrary complex number which is sent to its physical value $d = 3$ only at the end of the calculation. This "skeletonized" effective action approach to the motion of compact bodies has been extended to other theories of gravity [50, 51]. Finite-size corrections can be taken into account by adding nonminimal world line couplings to the effective action (2.7) [58, 59].

As we shall further discuss below, in the case of coalescing BNS systems, finite-size corrections (linked to tidal interactions) become relevant during late inspiral and must be included to accurately describe the dynamics of coalescing neutron stars.

Here, we shall not try to describe the results of the application of the multichart method to N-body (or two-body) systems. For applications to the solar system see the book by Brumberg [60]; see also several articles (notably by Soffel) in [61]. For applications of this method to binary pulsar systems (and to their use as tests of gravity theories) see the articles by Damour and Kramer in [62].

3 EOB description of the conservative dynamics of two-body systems

Before reviewing some of the technical aspects of the EOB method, let us indicate the historical roots of this method. First, we note that the EOB approach comprises three, rather separate, ingredients:

(1) a description of the conservative (Hamiltonian) part of the dynamics of two bodies;
(2) an expression for the radiation-reaction part of the dynamics;
(3) a description of the GW waveform emitted by a coalescing binary system.

For each one of these ingredients, the essential inputs that are used in EOB works are high-order PN expanded results which have been obtained by many years of work, by many researchers (see the review [46]). However, one of the key ideas in the EOB philosophy is to avoid using PN results in their original "Taylor-expanded" form (i.e. $c_0 + c_1 v/c + c_2 v^2/c^2 + c_3 v^3/c^3 + \cdots + c_n v^n/c^n$), but to use them instead in some *resummed* form (i.e. some nonpolynomial function of v/c, defined so as to incorporate some of the expected nonperturbative features of the exact result). The basic ideas and techniques for resumming each ingredient of the EOB are different and have different historical roots.

Concerning the first ingredient, i.e. the EOB Hamiltonian, it was inspired by an approach to electromagnetically interacting quantum two-body systems introduced by Brézin et al. [63].

The resummation of the second ingredient, i.e. the EOB radiation-reaction force $\mathcal{F}$, was initially inspired by the Padé resummation of the flux function introduced by Damour et al. [64]. More recently, a new and more sophisticated resummation technique for the (waveform and the) radiation reaction force $\mathcal{F}$ has been introduced by Damour et al. [65, 66]. It will be discussed in detail below.

As for the third ingredient, i.e. the EOB description of the waveform emitted by a coalescing black hole binary, it was mainly inspired by the work of Davis et al. [67] which discovered the transition between the plunge signal and a ringing tail when a particle falls into a black hole. Additional motivation for the EOB treatment of the transition from plunge to ring-down came from work on the, so-called close limit approximation [68].

Within the usual PN formalism, the conservative dynamics of a two-body system is currently fully known up to the 3PN level [19–24] (see below for the partial knowledge beyond the 3PN level). Going to the center of mass of the system ($\boldsymbol{p}_1 + \boldsymbol{p}_2 = 0$), the 3PN-accurate Hamiltonian (in Arnowitt–Deser–Misner-type coordinates) describing the relative motion, $\boldsymbol{q} = \boldsymbol{q}_1 - \boldsymbol{q}_2$, $\boldsymbol{p} = \boldsymbol{p}_1 = -\boldsymbol{p}_2$, has the structure

$$H_{3\mathrm{PN}}^{\mathrm{relative}}(\boldsymbol{q}, \boldsymbol{p}) = H_0(\boldsymbol{q}, \boldsymbol{p}) + \frac{1}{c^2} H_2(\boldsymbol{q}, \boldsymbol{p}) + \frac{1}{c^4} H_4(\boldsymbol{q}, \boldsymbol{p}) + \frac{1}{c^6} H_6(\boldsymbol{q}, \boldsymbol{p}) \,, \tag{3.1}$$

where

$$H_0(\boldsymbol{q}, \boldsymbol{p}) = \frac{1}{2\mu} \boldsymbol{p}^2 - \frac{GM\mu}{|\boldsymbol{q}|} \,, \tag{3.2}$$

with

$$M \equiv m_1 + m_2 \quad \text{and} \quad \mu \equiv m_1 m_2/M \,, \tag{3.3}$$

corresponds to the Newtonian approximation to the relative motion, while H_2 describes 1PN corrections, H_4 2PN ones and H_6 3PN ones. In terms of the rescaled variables $\boldsymbol{q}' \equiv \boldsymbol{q}/GM$, $\boldsymbol{p}' \equiv \boldsymbol{p}/\mu$, the explicit form (after dropping the primes for readability) of the 3PN-accurate rescaled Hamiltonian $\widehat{H} \equiv H/\mu$ reads [21, 70, 71]

$$\widehat{H}_N(\boldsymbol{q}, \boldsymbol{p}) = \frac{\boldsymbol{p}^2}{2} - \frac{1}{q}, \tag{3.4}$$

$$\widehat{H}_{1\mathrm{PN}}(\boldsymbol{q}, \boldsymbol{p}) = \frac{1}{8}(3\nu - 1)(\boldsymbol{p}^2)^2 - \frac{1}{2}\left[(3+\nu)\boldsymbol{p}^2 + \nu(\boldsymbol{n}\cdot\boldsymbol{p})^2\right]\frac{1}{q} + \frac{1}{2q^2}, \tag{3.5}$$

$$\begin{aligned}\widehat{H}_{2\mathrm{PN}}(\boldsymbol{q}, \boldsymbol{p}) = {} & \frac{1}{16}(1 - 5\nu + 5\nu^2)(\boldsymbol{p}^2)^3 \\ & + \frac{1}{8}\left[(5 - 20\nu - 3\nu^2)(\boldsymbol{p}^2)^2 - 2\nu^2(\boldsymbol{n}\cdot\boldsymbol{p})^2\boldsymbol{p}^2 - 3\nu^2(\boldsymbol{n}\cdot\boldsymbol{p})^4\right]\frac{1}{q} \\ & + \frac{1}{2}\left[(5+8\nu)\boldsymbol{p}^2 + 3\nu(\boldsymbol{n}\cdot\boldsymbol{p})^2\right]\frac{1}{q^2} - \frac{1}{4}(1+3\nu)\frac{1}{q^3},\end{aligned} \tag{3.6}$$

$$\begin{aligned}\widehat{H}_{3\mathrm{PN}}(\boldsymbol{q}, \boldsymbol{p}) = {} & \frac{1}{128}(-5 + 35\nu - 70\nu^2 + 35\nu^3)(\boldsymbol{p}^2)^4 \\ & + \frac{1}{16}\left[(-7 + 42\nu - 53\nu^2 - 5\nu^3)(\boldsymbol{p}^2)^3 + (2 - 3\nu)\nu^2(\boldsymbol{n}\cdot\boldsymbol{p})^2(\boldsymbol{p}^2)^2\right. \\ & \left. + 3(1-\nu)\nu^2(\boldsymbol{n}\cdot\boldsymbol{p})^4\boldsymbol{p}^2 - 5\nu^3(\boldsymbol{n}\cdot\boldsymbol{p})^6\right]\frac{1}{q} \\ & + \left[\frac{1}{16}(-27 + 136\nu + 109\nu^2)(\boldsymbol{p}^2)^2 + \frac{1}{16}(17 + 30\nu)\nu(\boldsymbol{n}\cdot\boldsymbol{p})^2\boldsymbol{p}^2\right. \\ & \left. + \frac{1}{12}(5 + 43\nu)\nu(\boldsymbol{n}\cdot\boldsymbol{p})^4\right]\frac{1}{q^2} \\ & + \left\{\left[-\frac{25}{8} + \left(\frac{1}{64}\pi^2 - \frac{335}{48}\right)\nu - \frac{23}{8}\nu^2\right]\boldsymbol{p}^2\right. \\ & \left. + \left(-\frac{85}{16} - \frac{3}{64}\pi^2 - \frac{7}{4}\nu\right)\nu(\boldsymbol{n}\cdot\boldsymbol{p})^2\right\}\frac{1}{q^3} \\ & + \left[\frac{1}{8} + \left(\frac{109}{12} - \frac{21}{32}\pi^2\right)\nu\right]\frac{1}{q^4}.\end{aligned} \tag{3.7}$$

In these formulas ν denotes the symmetric mass ratio:

$$\nu \equiv \frac{\mu}{M} \equiv \frac{m_1 m_2}{(m_1 + m_2)^2}. \tag{3.8}$$

The dimensionless parameter ν varies between 0 (extreme mass ratio case) and $\frac{1}{4}$ (equal mass case) and plays the rôle of a deformation parameter away from the test-mass limit.

It is well known that, at the Newtonian approximation, $H_0(\boldsymbol{q}, \boldsymbol{p})$ can be thought of as describing a "test particle" of mass μ orbiting around an "external mass" GM. The EOB approach is a *general relativistic generalization* of this fact. It consists in looking for an "effective external spacetime geometry" $g_{\mu\nu}^{\mathrm{eff}}(x^\lambda; GM, \nu)$ such that the geodesic dynamics of a "test particle" of mass μ within $g_{\mu\nu}^{\mathrm{eff}}(x^\lambda, GM, \nu)$ is *equivalent* (when expanded in powers of $1/c^2$) to the original, relative PN-expanded dynamics (3.1).

Let us explain the idea, proposed in [39], for establishing a "dictionary" between the real relative-motion dynamics, (3.1), and the dynamics of an "effective" particle of mass μ moving in $g^{\text{eff}}_{\mu\nu}(x^\lambda, GM, \nu)$. The idea consists in "thinking quantum mechanically"[1]. Instead of thinking in terms of a classical Hamiltonian, $H(\boldsymbol{q}, \boldsymbol{p})$ (such as $H^{\text{relative}}_{\text{3PN}}$, Equation (3.1)), and of its classical bound orbits, we can think in terms of the quantized energy levels $E(n, \ell)$ of the quantum bound states of the Hamiltonian operator $H(\hat{\boldsymbol{q}}, \hat{\boldsymbol{p}})$. These energy levels will depend on two (integer valued) quantum numbers n and ℓ. Here (for a spherically symmetric interaction, as appropriate to H^{relative}), ℓ parameterizes the total orbital angular momentum ($\boldsymbol{L}^2 = \ell(\ell+1)\,\hbar^2$), while n represents the "principal quantum number" $n = \ell + n_r + 1$, where n_r (the "radial quantum number") denotes the number of nodes in the radial wave function. The third "magnetic quantum number" m (with $-\ell \leq m \leq \ell$) does not enter the energy levels because of the spherical symmetry of the two-body interaction (in the center of of mass frame). For instance, the nonrelativistic Newton interaction (Equation (3.2)) gives rise to the well-known result

$$E_0(n, \ell) = -\frac{1}{2}\,\mu\left(\frac{GM\mu}{n\hbar}\right)^2 , \tag{3.9}$$

which depends only on n (this is the famous Coulomb degeneracy). When considering the PN corrections to H_0, as in Equation (3.1), one gets a more complicated expression of the form

$$\begin{aligned} E^{\text{relative}}_{\text{3PN}}(n, \ell) = -\frac{1}{2}\mu\frac{\alpha^2}{n^2}\Bigg[1 &+ \frac{\alpha^2}{c^2}\left(\frac{c_{11}}{n\ell} + \frac{c_{20}}{n^2}\right) \\ &+ \frac{\alpha^4}{c^4}\left(\frac{c_{13}}{n\ell^3} + \frac{c_{22}}{n^2\ell^2} + \frac{c_{31}}{n^3\ell} + \frac{c_{40}}{n^4}\right) + \frac{\alpha^6}{c^6}\left(\frac{c_{15}}{n\ell^5} + \cdots + \frac{c_{60}}{n^6}\right)\Bigg] , \end{aligned} \tag{3.10}$$

where we have set $\alpha \equiv GM\mu/\hbar = G\,m_1\,m_2/\hbar$, and where we consider, for simplicity, the (quasi-classical) limit where n and ℓ are large numbers. The 2PN-accurate version of Equation (3.10) had been derived by Damour and Schäfer [69] as early as 1988 while its 3PN-accurate version was derived by Damour et al. in 1999 [70]. The dimensionless coefficients c_{pq} are functions of the symmetric mass ratio $\nu \equiv \mu/M$, for instance $c_{40} = \frac{1}{8}(145 - 15\nu + \nu^2)$. In classical mechanics (i.e. for large n and ℓ), it is called the "Delaunay Hamiltonian," i.e. the Hamiltonian expressed in terms of the *action variables*[2] $J = \ell\hbar = \frac{1}{2\pi}\oint p_\varphi\, d\varphi$, and $N = n\hbar = I_r + J$, with $I_r = \frac{1}{2\pi}\oint p_r\, dr$.

The energy levels (3.10) encode, in a *gauge-invariant* way, the 3PN-accurate relative dynamics of a "real" binary. Let us now consider an auxiliary problem: the "effective" dynamics of one body, of mass μ, following (modulo the Q term discussed below)

1 This is related to an idea emphasized many times by John Archibald Wheeler: quantum mechanics can often help us in going to the essence of classical mechanics.

2 We consider, for simplicity, "equatorial" motions with $m = \ell$, i.e. classically, $\theta = \frac{\pi}{2}$.

a geodesic in some ν-dependent "effective external" (spherically symmetric) metric[3]

$$g_{\mu\nu}^{\text{eff}}\,dx^\mu\,dx^\nu = -A(R;\nu)\,c^2\,dT^2 + B(R;\nu)\,dR^2 + R^2(d\theta^2 + \sin^2\theta\,d\varphi^2)\,. \tag{3.11}$$

Here, the *a priori unknown* metric functions $A(R;\nu)$ and $B(R;\nu)$ will be constructed in the form of expansions in GM/c^2R:

$$\begin{aligned} A(R;\nu) &= 1 + \tilde{a}_1\,\frac{GM}{c^2R} + \tilde{a}_2\left(\frac{GM}{c^2R}\right)^2 + \tilde{a}_3\left(\frac{GM}{c^2R}\right)^3 + \tilde{a}_4\left(\frac{GM}{c^2R}\right)^4 + \cdots\,; \\ B(R;\nu) &= 1 + \tilde{b}_1\,\frac{GM}{c^2R} + \tilde{b}_2\left(\frac{GM}{c^2R}\right)^2 + b_3\left(\frac{GM}{c^2R}\right)^3 + \cdots\,, \end{aligned} \tag{3.12}$$

where the dimensionless coefficients $\tilde{a}_n, \tilde{b}_n$ depend on ν. From the Newtonian limit, it is clear that we should set $\tilde{a}_1 = -2$. In addition, as ν can be viewed as a deformation parameter away from the test-mass limit, we require that the effective metric (3.11) tend to the Schwarzschild metric (of mass M) as $\nu \to 0$, that is

$$A(R;\nu=0) = 1 - 2GM/c^2R = B^{-1}(R;\nu=0)\,.$$

Let us now require that the dynamics of the "one body" μ within the effective metric $g_{\mu\nu}^{\text{eff}}$ be described by an "effective" mass-shell condition of the form

$$g_{\text{eff}}^{\mu\nu}\,p_\mu^{\text{eff}}\,p_\nu^{\text{eff}} + \mu^2\,c^2 + Q(p_\mu^{\text{eff}}) = 0\,,$$

where $Q(p)$ is (at least) *quartic* in p. Then by solving (by separation of variables) the corresponding "effective" Hamilton–Jacobi equation

$$\begin{aligned} g_{\text{eff}}^{\mu\nu}\,\frac{\partial S_{\text{eff}}}{\partial x^\mu}\,\frac{\partial S_{\text{eff}}}{\partial x^\nu} + \mu^2 c^2 + Q\left(\frac{\partial S_{\text{eff}}}{\partial x^\mu}\right) &= 0\,, \\ S_{\text{eff}} = -\mathcal{E}_{\text{eff}}\,t + J_{\text{eff}}\,\varphi + S_{\text{eff}}(R)\,, \end{aligned} \tag{3.13}$$

one can straightforwardly compute (in the quasi-classical, large quantum numbers limit) the effective Delaunay Hamiltonian $\mathcal{E}_{\text{eff}}(N_{\text{eff}}, J_{\text{eff}})$, with $N_{\text{eff}} = n_{\text{eff}}\,\hbar$, $J_{\text{eff}} = \ell_{\text{eff}}\,\hbar$ (where $N_{\text{eff}} = J_{\text{eff}} + I_R^{\text{eff}}$, with $I_R^{\text{eff}} = \frac{1}{2\pi}\oint p_R^{\text{eff}}\,dR$, $P_R^{\text{eff}} = \partial S_{\text{eff}}(R)/dR$). This yields a result of the form

$$\begin{aligned} \mathcal{E}_{\text{eff}}(n_{\text{eff}}, \ell_{\text{eff}}) = \mu c^2 - \frac{1}{2}\,\mu\,\frac{\alpha^2}{n_{\text{eff}}^2}\Bigg[1 &+ \frac{\alpha^2}{c^2}\left(\frac{c_{11}^{\text{eff}}}{n_{\text{eff}}\ell_{\text{eff}}} + \frac{c_{20}^{\text{eff}}}{n_{\text{eff}}^2}\right) \\ &+ \frac{\alpha^4}{c^4}\left(\frac{c_{13}^{\text{eff}}}{n_{\text{eff}}\ell_{\text{eff}}^3} + \frac{c_{22}^{\text{eff}}}{n_{\text{eff}}^2\ell_{\text{eff}}^2} + \frac{c_{31}^{\text{eff}}}{n_{\text{eff}}^3\ell_{\text{eff}}} + \frac{c_{40}^{\text{eff}}}{n_{\text{eff}}^4}\right) \\ &+ \frac{\alpha^6}{c^6}\left(\frac{c_{15}^{\text{eff}}}{n_{\text{eff}}\ell_{\text{eff}}^5} + \cdots + \frac{c_{60}^{\text{eff}}}{n_{\text{eff}}^6}\right)\Bigg]\,, \end{aligned} \tag{3.14}$$

3 It is convenient to write the "effective metric" in Schwarzschild-like coordinates. Note that the effective radial coordinate R differs from the two-body ADM-coordinate relative distance $R^{\text{ADM}} = |\boldsymbol{q}|$. The transformation between the two coordinate systems has been determined in Refs. [39, 41].

where the dimensionless coefficients $c^{\rm eff}_{pq}$ are now functions of the unknown coefficients $\widetilde{a}_n, \widetilde{b}_n$ entering the looked for "external" metric coefficients (3.12).

At this stage, one needs to define a "dictionary" between the real (relative) two-body dynamics, summarized in Equation (3.10), and the effective one-body one, summarized in Equation (3.14). As, on both sides, quantum mechanics tells us that the action variables are quantized in integers ($N_{\rm real} = n\hbar$, $N_{\rm eff} = n_{\rm eff}\hbar$, etc.) it is most natural to identify $n = n_{\rm eff}$ and $\ell = \ell_{\rm eff}$. One then still needs a rule for relating the two different energies $E^{\rm relative}_{\rm real}$ and $\mathcal{E}_{\rm eff}$. Buonanno and Damour [39] proposed to look for a general map between the real energy levels and the effective ones (which, as seen when comparing (3.10) and (3.14), cannot be directly identified because they do not include the same rest-mass contribution[4]), namely

$$\frac{\mathcal{E}_{\rm eff}}{\mu c^2} - 1 = f\left(\frac{E^{\rm relative}_{\rm real}}{\mu c^2}\right) = \frac{E^{\rm relative}_{\rm real}}{\mu c^2}\left(1 + \alpha_1 \frac{E^{\rm relative}_{\rm real}}{\mu c^2} + \alpha_2 \left(\frac{E^{\rm relative}_{\rm real}}{\mu c^2}\right)^2 \right.$$
$$\left. + \alpha_3 \left(\frac{E^{\rm relative}_{\rm real}}{\mu c^2}\right)^3 + \cdots \right) . \tag{3.15}$$

The "correspondence" between the real and effective energy levels is illustrated in Figure 1.

Finally, identifying $\mathcal{E}_{\rm eff}(n,\ell)/\mu c^2$ to $1 + f(E^{\rm relative}_{\rm real}(n,\ell)/\mu c^2)$ yields a system of equations for determining the unknown EOB coefficients $\widetilde{a}_n, \widetilde{b}_n, \alpha_n$, as well as the three coefficients z_1, z_2, z_3 parameterizing a general 3PN-level quartic mass-shell deformation:

$$Q_{\rm 3PN}(p) = \frac{1}{c^6}\frac{1}{\mu^2}\left(\frac{GM}{R}\right)^2 \left[z_1\, \boldsymbol{p}^4 + z_2\, \boldsymbol{p}^2 (\boldsymbol{n}\cdot\boldsymbol{p})^2 + z_3 (\boldsymbol{n}\cdot\boldsymbol{p})^4\right] .$$

[The need for introducing a quartic mass-shell deformation Q only arises at the 3PN level.]

The above system of equations for $\widetilde{a}_n, \widetilde{b}_n, \alpha_n$ (and z_i at 3PN) was studied at the 2PN level in Ref. [39], and at the 3PN level in Ref. [41]. At the 2PN level it was found that, if one further imposes the natural condition $\widetilde{b}_1 = +2$ (so that the linearized effective metric coincides with the linearized Schwarzschild metric with mass $M = m_1 + m_2$), there exists a *unique* solution for the remaining five unknown coefficients $\widetilde{a}_2, \widetilde{a}_3, \widetilde{b}_2, \alpha_1$ and α_2. This solution is very simple:

$$\widetilde{a}_2 = 0\,, \quad \widetilde{a}_3 = 2\nu\,, \quad \widetilde{b}_2 = 4 - 6\nu\,, \quad \alpha_1 = \frac{\nu}{2}\,, \quad \alpha_2 = 0\,. \tag{3.16}$$

At the 3PN level, it was found that the system of equations is consistent, and underdetermined in that the general solution can be parameterized by the arbitrary values of

4 Indeed $E^{\rm total}_{\rm real} = Mc^2 + E^{\rm relative}_{\rm real} = Mc^2 + \text{Newtonian terms} + 1\text{PN}/c^2 + \cdots$, while $\mathcal{E}_{\rm effective} = \mu c^2 + N + 1\text{PN}/c^2 + \cdots$.

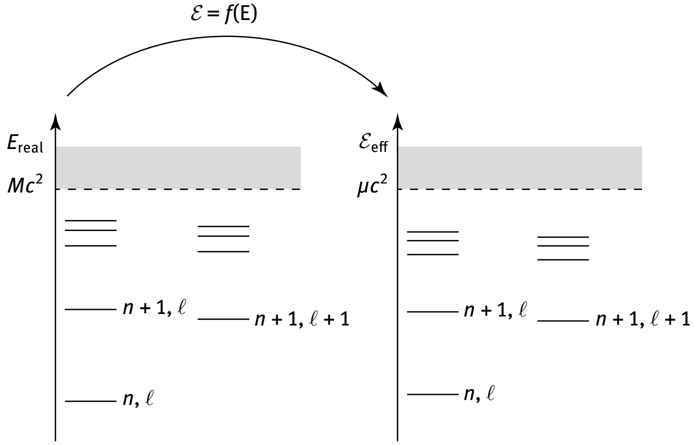

Fig. 1. Sketch of the correspondence between the quantized energy levels of the real and effective conservative dynamics. n denotes the "principal quantum number" ($n = n_r + \ell + 1$, with $n_r = 0, 1, \ldots$ denoting the number of nodes in the radial function), while ℓ denotes the (relative) orbital angular momentum ($\boldsymbol{L}^2 = \ell(\ell + 1)\,\hbar^2$). Though the EOB method is purely classical, it is conceptually useful to think in terms of the underlying (Bohr–Sommerfeld) quantization conditions of the action variables I_R and J to motivate the identification between n and ℓ in the two dynamics.

z_1 and z_2. It was then argued that it is natural to impose the simplifying requirements $z_1 = 0 = z_2$, so that Q is proportional to the fourth power of the (effective) radial momentum p_r. With these conditions, the solution is unique at the 3PN level, and is still remarkably simple, namely

$$\widetilde{a}_4 = a_4\,\nu\,,\ \widetilde{d}_3 = 2(3\nu - 26)\nu\,,\ \alpha_3 = 0\,,\ z_3 = 2(4 - 3\nu)\nu\,.$$

Here, a_4 denotes the number

$$a_4 = \frac{94}{3} - \frac{41}{32}\pi^2 \simeq 18.6879027 \tag{3.17}$$

while $\widetilde{d}_3$ denotes the coefficient of $(GM/c^2R)^3$ in the PN expansion of the combined metric coefficient

$$D(R) \equiv A(R)\,B(R)\,.$$

Replacing $B(R)$ by $D(R)$ is convenient because (as mentioned above), in the test-mass limit $\nu \to 0$, the effective metric must reduce to the Schwarzschild metric, namely

$$A(R;\nu = 0) = B^{-1}(R;\nu = 0) = 1 - 2\left(\frac{GM}{c^2R}\right)\,,$$

so that

$$D(R;\nu = 0) = 1\,.$$

The final result is that the three EOB potentials A, D, Q describing the 3PN two-body dynamics are given by the following very simple results. In terms of the EOB "gravitational potential"

$$u \equiv \frac{GM}{c^2R},$$

$$A_{3\mathrm{PN}}(R) = 1 - 2u + 2\,\nu\,u^3 + a_4\,\nu\,u^4\,, \tag{3.18}$$

$$D_{3\mathrm{PN}}(R) \equiv (A(R)B(R))_{3\mathrm{PN}} = 1 - 6\nu u^2 + 2(3\nu - 26)\nu u^3\,, \tag{3.19}$$

$$Q_{3\mathrm{PN}}(\boldsymbol{q}, \boldsymbol{p}) = \frac{1}{c^2}\,2(4 - 3\nu)\nu\,u^2\,\frac{p_r^4}{\mu^2}\,. \tag{3.20}$$

In addition, the map between the (real) center-of-mass energy of the binary system $E_{\mathrm{real}}^{\mathrm{relative}} = H^{\mathrm{relative}} = \mathcal{E}_{\mathrm{relative}}^{\mathrm{tot}} - Mc^2$ and the effective one $\mathcal{E}_{\mathrm{eff}}$ is found to have the very simple (but nontrivial) form

$$\frac{\mathcal{E}_{\mathrm{eff}}}{\mu c^2} = 1 + \frac{E_{\mathrm{real}}^{\mathrm{relative}}}{\mu c^2}\left(1 + \frac{\nu}{2}\,\frac{E_{\mathrm{real}}^{\mathrm{relative}}}{\mu c^2}\right) = \frac{s - m_1^2\,c^4 - m_2^2\,c^4}{2\,m_1\,m_2\,c^4} \tag{3.21}$$

where $s = (\mathcal{E}_{\mathrm{real}}^{\mathrm{tot}})^2 \equiv (Mc^2 + E_{\mathrm{real}}^{\mathrm{relative}})^2$ is Mandelstam's invariant $s = -(p_1 + p_2)^2$.

It is truly remarkable that the EOB formalism succeeds in *condensing* the complicated, original 3PN Hamiltonian, Equations (3.4)–(3.7), into the very simple potentials A, D, and Q displayed above, together with the simple energy map Equation (3.21). For instance, at the 1PN level, the already somewhat involved Lorentz–Droste–Einstein–Infeld–Hoffmann 1PN dynamics (Equations (3.4) and (3.5)) is simply described, within the EOB formalism, as a test particle of mass μ moving in an external Schwarzschild background of mass $M = m_1 + m_2$, together with the (crucial but quite simple) energy transformation (3.21). (Indeed, the ν-dependent corrections to A and D start only at the 2PN level.) At the 2PN level, the seven rather complicated ν-dependent coefficients of $\widehat{H}_{2\mathrm{PN}}(\boldsymbol{q}, \boldsymbol{p})$, Equation (3.6), get condensed into the two very simple additional contributions $+\,2\nu u^3$ in $A(u)$, and $-\,6\nu u^2$ in $D(u)$. At the 3PN level, the 11 quite complicated ν-dependent coefficients of $\widehat{H}_{3\mathrm{PN}}$, Equation (3.7), get condensed into only three simple contributions: $+\,a_4\nu u^4$ in $A(u)$, $+\,2(3\nu - 26)\nu u^3$ in $D(u)$, and $Q_{3\mathrm{PN}}$ given by Equation (3.20). This simplicity of the EOB results is not only due to the reformulation of the PN-expanded Hamiltonian into an effective dynamics. Notably, the A-potential is much simpler that it could a priori have been: (i) as already noted it is not modified at the 1PN level, while one would a priori expect to have found a 1PN potential $A_{1\mathrm{PN}}(u) = 1 - 2u + \nu a_2 u^2$ with some nonzero a_2; and (ii) there are striking cancellations taking place in the calculation of the 2PN and 3PN coefficients $\tilde{a}_2(\nu)$ and $\tilde{a}_3(\nu)$, which were a priori of the form $\tilde{a}_2(\nu) = a_2\nu + a_2'\nu^2$, and $\tilde{a}_3(\nu) = a_3\nu + a_3'\nu^2 + a_3''\nu^3$, but for which the ν-nonlinear contributions $a_2'\nu^2, a_3'\nu^2$ and $a_3''\nu^3$ precisely canceled out. Similar cancellations take place at the 4PN level (level at which it was recently possible to compute the A-potential, see below). Let us note for completeness that, starting at the 4PN level, the Taylor expansions of the A and D potentials depend on the logarithm of u. The corresponding logarithmic contributions have been computed at the 4PN level [72, 73] and even the 5PN one [74, 75]. They have been incorporated in a recent, improved implementation of the EOB formalism [76].

The fact that the 3PN coefficient a_4 in the crucial "effective radial potential" $A_{3PN}(R)$, Equation (3.18), is rather large and positive indicates that the ν-dependent nonlinear gravitational effects lead, for comparable masses ($\nu \sim \frac{1}{4}$), to a last stable (circular) orbit (LSO) which has a higher frequency and a larger binding energy than what a naive scaling from the test-particle limit ($\nu \to 0$) would suggest. Actually, the PN-expanded form (3.18) of $A_{3PN}(R)$ does not seem to be a good representation of the (unknown) exact function $A_{EOB}(R)$ when the (Schwarzschild-like) relative coordinate R becomes smaller than about $6GM/c^2$ (which is the radius of the LSO in the test-mass limit). In fact, by continuity with the test-mass case, one a priori expects that $A_{3PN}(R)$ always exhibits a simple zero defining an EOB "effective horizon" that is smoothly connected to the Schwarzschild event horizon at $R = 2GM/c^2$ when $\nu \to 0$. However, the large value of the a_4 coefficient does actually prevent A_{3PN} to have this property when ν is too large, and in particular when $\nu = 1/4$. It was therefore suggested [41] to further resum[5] $A_{3PN}(R)$ by replacing it by a suitable Padé (P) approximant. For instance, the replacement of $A_{3PN}(R)$ by[6]

$$A_3^1(R) \equiv P_3^1\left(A_{3PN}(R)\right) = \frac{1 + n_1 u}{1 + d_1 u + d_2 u^2 + d_3 u^3} \tag{3.22}$$

ensures that the $\nu = \frac{1}{4}$ case is smoothly connected with the $\nu = 0$ limit.

The same kind of ν-continuity argument, discussed so far for the A function, needs to be applied also to the $D_{3PN}(R)$ function defined in Equation (3.19). A straightforward way to ensure that the D function stays positive when R decreases (since it is $D = 1$ when $\nu \to 0$) is to replace $D_{3PN}(R)$ by $D_3^0(R) \equiv P_3^0[D_{3PN}(R)]$, where P_3^0 indicates the $(0, 3)$ Padé approximant and explicitly reads

$$D_3^0(R) = \frac{1}{1 + 6\nu u^2 - 2(3\nu - 26)\nu u^3} . \tag{3.23}$$

5 The PN-expanded EOB building blocks $A_{3PN}(R), B_{3PN}(R), \ldots$ already represent a *resummation* of the PN dynamics in the sense that they have "condensed" the many terms of the original PN-expanded Hamiltonian within a very concise format. But one should not refrain to further resum the EOB building blocks themselves, if this is physically motivated.

6 We recall that the coefficients n_1 and (d_1, d_2, d_3) of the $(1, 3)$ Padé approximant $P_3^1(A_{3PN}(u))$ are determined by the condition that the first four terms of the Taylor expansion of A_3^1 in powers of $u = GM/(c^2R)$ coincide with A_{3PN}.

4 EOB description of radiation reaction and of the emitted waveform during inspiral

In the previous section, we have described how the EOB method encodes the conservative part of the relative orbital dynamics into the dynamics of an "effective" particle. Let us now briefly discuss how to complete the EOB dynamics by defining some *resummed* expressions describing radiation reaction effects, and the corresponding waveform emitted at infinity. One is interested in circularized binaries, which have lost their initial eccentricity under the influence of radiation reaction. For such systems, it is enough (in the first approximation [40]; see, however, the recent results of Bini and Damour [77]) to include a radiation reaction force in the p_φ equation of motion only. More precisely, we are using phase space variables $r, p_r, \varphi, p_\varphi$ associated to polar coordinates (in the equatorial plane $\theta = \frac{\pi}{2}$). Actually it is convenient to replace the radial momentum p_r by the momentum conjugate to the "tortoise" radial coordinate $R_* = \int dR(B/A)^{1/2}$, i.e. $P_{R_*} = (A/B)^{1/2} P_R$. The real EOB Hamiltonian is obtained by first solving Equation (3.21) to get $H_{\rm real}^{\rm total} = \sqrt{s}$ in terms of $\mathcal{E}_{\rm eff}$, and then by solving the effective Hamilton–Jacobi equation to get $\mathcal{E}_{\rm eff}$ in terms of the effective phase space coordinates $\boldsymbol{q}_{\rm eff}$ and $\boldsymbol{p}_{\rm eff}$. The result is given by two nested square roots (we henceforth set $c = 1$):

$$\hat{H}_{\rm EOB}(r, p_{r_*}, \varphi) = \frac{H_{\rm EOB}^{\rm real}}{\mu} = \frac{1}{\nu}\sqrt{1 + 2\nu\,(\hat{H}_{\rm eff} - 1)}\,, \tag{4.1}$$

where

$$\hat{H}_{\rm eff} = \sqrt{p_{r_*}^2 + A(r)\left(1 + \frac{p_\varphi^2}{r^2} + z_3\,\frac{p_{r_*}^4}{r^2}\right)}\,, \tag{4.2}$$

with $z_3 = 2\nu\,(4 - 3\nu)$. Here, we are using suitably rescaled dimensionless (effective) variables: $r = R/GM$, $p_{r_*} = P_{R_*}/\mu$, $p_\varphi = P_\varphi/\mu GM$, as well as a rescaled time $t = T/GM$. This leads to equations of motion for $(r, \varphi, p_{r_*}, p_\varphi)$ of the form

$$\frac{d\varphi}{dt} = \frac{\partial \hat{H}_{\rm EOB}}{\partial p_\varphi} \equiv \Omega\,, \tag{4.3}$$

$$\frac{dr}{dt} = \left(\frac{A}{B}\right)^{1/2} \frac{\partial \hat{H}_{\rm EOB}}{\partial p_{r_*}}\,, \tag{4.4}$$

$$\frac{dp_\varphi}{dt} = \hat{\mathcal{F}}_\varphi\,, \tag{4.5}$$

$$\frac{dp_{r_*}}{dt} = -\left(\frac{A}{B}\right)^{1/2} \frac{\partial \hat{H}_{\rm EOB}}{\partial r}\,, \tag{4.6}$$

which explicitly read

$$\frac{d\varphi}{dt} = \frac{Ap_\varphi}{\nu r^2 \hat{H}\hat{H}_{\mathrm{eff}}} \equiv \Omega \tag{4.7}$$

$$\frac{dr}{dt} = \left(\frac{A}{B}\right)^{1/2} \frac{1}{\nu \hat{H}\hat{H}_{\mathrm{eff}}} \left(p_{r_*} + z_3 \frac{2A}{r^2} p_{r_*}^3\right) \tag{4.8}$$

$$\frac{dp_\varphi}{dt} = \hat{\mathfrak{F}}_\varphi \tag{4.9}$$

$$\frac{dp_{r_*}}{dt} = -\left(\frac{A}{B}\right)^{1/2} \frac{1}{2\nu \hat{H}\hat{H}_{\mathrm{eff}}} \left\{A' + \frac{p_\varphi^2}{r^2}\left(A' - \frac{2A}{r}\right) + z_3\left(\frac{A'}{r^2} - \frac{2A}{r^3}\right)p_{r_*}^4\right\} , \tag{4.10}$$

where $A' = dA/dr$. As explained above the EOB metric function $A(r)$ is defined by Padé resumming the Taylor-expanded result (3.12) obtained from the matching between the real and effective energy levels (as we were mentioning, one uses a similar Padé resumming for $D(r) \equiv A(r)\,B(r)$). One similarly needs to resum $\hat{\mathfrak{F}}_\varphi$, i.e. the φ component of the radiation reaction which has been introduced on the right-hand side of Equation (4.5).

Several methods have been tried during the development of the EOB formalism to resum the radiation reaction $\widehat{\mathfrak{F}}_\varphi$ (starting from the high-order PN-expanded results that have been obtained in the literature). Here, we shall briefly explain the new, *parameter-free* resummation technique for the multipolar waveform (and thus for the energy flux) introduced in Refs. [78, 79] and perfected in [65]. To be precise, the new results discussed in Ref. [65] are twofold: on the one hand, that work generalized the $\ell = m = 2$ resummed factorized waveform of [78, 79] to higher multipoles by using the most accurate currently known PN-expanded results [80–83] as well as the higher PN terms which are known in the test-mass limit [84, 85]; on the other hand, it introduced a *new resummation procedure* which consists in considering a new theoretical quantity, denoted as $\rho_{\ell m}(x)$, which enters the (ℓ, m) waveform (together with other building blocks, see below) only through its ℓth power: $h_{\ell m} \propto (\rho_{\ell m}(x))^\ell$. Here, and below, x denotes the invariant PN-ordering parameter given during inspiral by $x \equiv (GM\Omega/c^3)^{2/3}$.

The main novelty introduced by Ref. [65] is to write the (ℓ, m) multipolar waveform emitted by a circular nonspinning compact binary as the *product* of several factors, namely

$$h_{\ell m}^{(\epsilon)} = \frac{GM\nu}{c^2 R} n_{\ell m}^{(\epsilon)} c_{\lambda+\epsilon}(\nu) x^{(\ell+\epsilon)/2} Y^{\ell-\epsilon,-m}\left(\frac{\pi}{2}, \Phi\right) \hat{S}_{\mathrm{eff}}^{(\epsilon)} T_{\ell m} e^{\mathrm{i}\delta_{\ell m}} \rho_{\ell m}^{\ell}. \tag{4.11}$$

Here ϵ denotes the parity of $\ell + m$ ($\epsilon = \pi(\ell + m)$), i.e. $\epsilon = 0$ for "even-parity" (mass-generated) multipoles ($\ell + m$ even), and $\epsilon = 1$ for "odd-parity" (current-generated) ones ($\ell + m$ odd); $n^{(\epsilon)}_{\ell m}$ and $c_{\lambda+\epsilon}(\nu)$ are numerical coefficients; $\hat{S}^{(\epsilon)}_{\text{eff}}$ is a μ-normalized effective source (whose definition comes from the EOB formalism); $T_{\ell m}$ is a resummed version [78, 79] of an infinite number of "leading logarithms" entering the *tail effects* [86, 87]; $\delta_{\ell m}$ is a supplementary phase (which corrects the phase effects not included in the *complex* tail factor $T_{\ell m}$), and, finally, $(\rho_{\ell m})^{\ell}$ denotes the ℓth power of the quantity $\rho_{\ell m}$ which is the new building block introduced in [65]. Note that in previous papers [78, 79] the quantity $(\rho_{\ell m})^{\ell}$ was denoted as $f_{\ell m}$ and we will often use this notation below. Before introducing explicitly the various elements entering the waveform (4.11) it is convenient to decompose $h_{\ell m}$ as

$$h^{(\epsilon)}_{\ell m} = h^{(N,\epsilon)}_{\ell m} \hat{h}^{(\epsilon)}_{\ell m}, \tag{4.12}$$

where $h^{(N,\epsilon)}_{\ell m}$ is the Newtonian contribution (i.e. the product of the first five factors in Equation (4.11)) and

$$\hat{h}^{(\epsilon)}_{\ell m} \equiv \hat{S}^{(\epsilon)}_{\text{eff}} T_{\ell m} e^{\mathrm{i}\delta_{\ell m}} f_{\ell m} \tag{4.13}$$

represents a resummed version of all the PN corrections. The PN correcting factor $\hat{h}^{(\epsilon)}_{\ell m}$, as well as all its building blocks, has the structure $\hat{h}^{(\epsilon)}_{\ell m} = 1 + \mathcal{O}(x)$.

The reader will find in Ref. [65] the definitions of the quantities entering the "Newtonian" waveform $h^{(N,\epsilon)}_{\ell m}$, as well as the precise definition of the effective source factor $\widehat{S}^{(\epsilon)}_{\text{eff}}$, which constitutes the first factor in the PN-correcting factor $\widehat{h}^{(\epsilon)}_{\ell m}$. Let us only note here that the definition of $\widehat{S}^{(\epsilon)}_{\text{eff}}$ makes use of EOB-defined quantities. For instance, for even-parity waves ($\epsilon = 0$) $\widehat{S}^{(0)}_{\text{eff}}$ is defined as the μ-scaled *effective* energy $\mathcal{E}_{\text{eff}}/\mu c^2$. (We use the "$J$-factorization" definition of $\widehat{S}^{(\epsilon)}_{\text{eff}}$ when $\epsilon = 1$, i.e. for odd parity waves.)

The second building block in the factorized decomposition is the "tail factor" $T_{\ell m}$ (introduced in Refs. [78, 79]). As mentioned above, $T_{\ell m}$ is a resummed version of an infinite number of "leading logarithms" entering the transfer function between the near-zone multipolar wave and the far-zone one, due to *tail effects* linked to its propagation in a Schwarzschild background of mass $M_{\text{ADM}} = H^{\text{real}}_{\text{EOB}}$. Its explicit expression reads

$$T_{\ell m} = \frac{\Gamma(\ell + 1 - 2\mathrm{i}\hat{\hat{k}})}{\Gamma(\ell + 1)} e^{\pi\hat{\hat{k}}} e^{2\mathrm{i}\hat{\hat{k}}\log(2kr_0)}, \tag{4.14}$$

where $r_0 = 2GM/\sqrt{e}$ and $\hat{\hat{k}} \equiv GH^{\text{real}}_{\text{EOB}} m\Omega$ and $k \equiv m\Omega$. Note that $\hat{\hat{k}}$ differs from k by a rescaling involving the *real* (rather than the *effective*) EOB Hamiltonian, computed at this stage along the sequence of circular orbits.

The tail factor $T_{\ell m}$ is a complex number which already takes into account some of the dephasing of the partial waves as they propagate out from the near zone to infinity. However, as the tail factor only takes into account the leading logarithms, one needs to correct it by a complementary dephasing term, $e^{\mathrm{i}\delta_{\ell m}}$, linked to subleading logarithms and other effects. This subleading phase correction can be computed as being the phase $\delta_{\ell m}$ of the complex ratio between the PN-expanded $\hat{h}^{(\epsilon)}_{\ell m}$ and the above defined source and tail factors. In the comparable-mass case ($\nu \neq 0$), the 3PN δ_{22} phase correction to the leading quadrupolar wave was originally computed in Ref. [79] (see also Ref. [78] for the $\nu = 0$ limit). Full results for the subleading partial waves to the highest possible PN-accuracy by starting from the currently known 3PN-accurate ν-dependent waveform [83] have been obtained in [65]. For higher order test-mass ($\nu \to 0$) contributions, see [88, 89]. For extensions of the (nonspinning) factorized waveform of [65] see [90–92].

The last factor in the multiplicative decomposition of the multipolar waveform can be computed as being the modulus $f_{\ell m}$ of the complex ratio between the PN-expanded $\hat{h}^{(\epsilon)}_{\ell m}$ and the above defined source and tail factors. In the comparable mass case ($\nu \neq 0$), the f_{22} modulus correction to the leading quadrupolar wave was computed in Ref. [79] (see also Ref. [78] for the $\nu = 0$ limit). For the subleading partial waves, Ref. [65] explicitly computed the other $f_{\ell m}$'s to the highest possible PN-accuracy by starting from the currently known 3PN-accurate ν-dependent waveform [83]. In addition, as originally proposed in Ref. [79], to reach greater accuracy the $f_{\ell m}(x;\nu)$'s extracted from the 3PN-accurate $\nu \neq 0$ results are completed by adding higher order contributions coming from the $\nu = 0$ results [84, 85]. In the particular f_{22} case discussed in [79], this amounted to adding 4PN and 5PN $\nu = 0$ terms. This "hybridization" procedure was then systematically pursued for all the other multipoles, using the 5.5PN accurate calculation of the multipolar decomposition of the gravitational wave energy flux of Refs. [84, 85].

The decomposition of the total PN-correction factor $\hat{h}^{(\epsilon)}_{\ell m}$ into several factors is in itself a resummation procedure which already improves the convergence of the PN series one has to deal with: indeed, one can see that the coefficients entering increasing powers of x in the PN expansion of the $f_{\ell m}$'s tend to be systematically smaller than the coefficients appearing in the usual PN expansion of $\hat{h}^{(\epsilon)}_{\ell m}$. The reason for this is essentially twofold: (i) the factorization of $T_{\ell m}$ has absorbed powers of $m\pi$ which contributed to make large coefficients in $\hat{h}^{(\epsilon)}_{\ell m}$, and (ii) the factorization of either $\hat{H}_{\text{eff}}$ or $\hat{j}$ has (in the $\nu = 0$ case) removed the presence of an inverse square-root singularity located at $x = 1/3$ which caused the coefficient of x^n in any PN-expanded quantity to grow as 3^n as $n \to \infty$.

To further improve the convergence of the waveform several resummations of the factor $f_{\ell m}(x) = 1 + c_1^{\ell m} x + c_2^{\ell m} x^2 + \cdots$ have been suggested. First, Refs. [78, 79] proposed to further resum the $f_{22}(x)$ function via a Padé (3,2) approximant, $P^3_2\{f_{22}(x;\nu)\}$, so as to improve its behavior in the strong-field-fast-motion regime. Such a resummation gave an excellent agreement with numerically computed waveforms, near the end of the inspiral and during the beginning of the plunge, for different mass ratios [78, 93, 94]. As we were mentioning above, a new route for resumming $f_{\ell m}$ was explored in Ref. [65]. It is based on replacing $f_{\ell m}$ by its ℓth root, say

$$\rho_{\ell m}(x;\nu) = [f_{\ell m}(x;\nu)]^{1/\ell}. \tag{4.15}$$

The basic motivation for replacing $f_{\ell m}$ by $\rho_{\ell m}$ is the following: the leading "Newtonian-level" contribution to the waveform $h^{(\epsilon)}_{\ell m}$ contains a factor $\omega^\ell r^\ell_{\text{harm}} v^\epsilon$, where r_{harm} is the harmonic radial coordinate used in the MPM formalism [95, 96]. When computing the PN expansion of this factor one has to insert the PN expansion of the (dimensionless) harmonic radial coordinate r_{harm}, $r_{\text{harm}} = x^{-1}(1 + c_1 x + \mathcal{O}(x^2))$, as a function of the gauge-independent frequency parameter x. The PN re-expansion of $[r_{\text{harm}}(x)]^\ell$ then generates terms of the type $x^{-\ell}(1 + \ell c_1 x + cdots)$. This is one (though not the only one) of the origins of 1PN corrections in $h_{\ell m}$ and $f_{\ell m}$ whose coefficients grow linearly with ℓ. The study of [65] has pointed out that these ℓ-growing terms are problematic for the accuracy of the PN-expansions. The replacement of $f_{\ell m}$ by $\rho_{\ell m}$ is a cure for this problem.

Several studies, both in the test-mass limit, $\nu \to 0$ (see Figure 1 in [65]) and in the comparable-mass case (see notably Figure 4 in [66]), have shown that the resummed factorized (inspiral) EOB waveforms defined above provided remarkably accurate analytical approximations to the "exact" inspiral waveforms computed by numerical simulations. These resummed multipolar EOB waveforms are much closer (especially during late inspiral) to the exact ones than the standard PN-expanded waveforms given by Equation (4.12) with a PN-correction factor of the usual "Taylor-expanded" form

$$\hat{h}^{(\epsilon)\text{PN}}_{\ell m} = 1 + c_1^{\ell m} x + c_{3/2}^{\ell m} x^{3/2} + c_2^{\ell m} x^2 + \cdots$$

See Figure 1 in [65].

Finally, one uses the newly resummed multipolar waveforms (4.11) to define a resummation of the *radiation reaction force* $\mathcal{F}_\varphi$ defined as

$$\mathcal{F}_\varphi = -\frac{1}{\Omega} F^{(\ell_{\max})}, \tag{4.16}$$

where the (instantaneous, circular) GW flux $F^{(\ell_{\max})}$ is defined as

$$F^{(\ell_{\max})} = \frac{2}{16\pi G} \sum_{\ell=2}^{\ell_{\max}} \sum_{m=1}^{\ell} (m\Omega)^2 |R h_{\ell m}|^2. \tag{4.17}$$

Summarizing: Equations (4.11) and (4.16), (4.17) define resummed EOB versions of the waveform $h_{\ell m}$, and of the radiation reaction $\widehat{\mathcal{F}}_\varphi$, during inspiral. A crucial point is that these resummed expressions are *parameter free*. Given some current approximation to the conservative EOB dynamics (i.e. some expressions for the A, D, Q potentials) they *complete* the EOB formalism by giving explicit predictions for the radiation reaction (thereby completing the dynamics, see Equations (4.3)–(4.6)), and for the emitted inspiral waveform.

5 EOB description of the merger of binary black holes and of the ringdown of the final black hole

Up to now we have reviewed how the EOB formalism, starting only from *analytical* information obtained from PN theory, and adding extra resummation requirements (both for the EOB conservative potentials A, Equation (3.22), and D, Equation (3.23), and for the waveform, Equation (4.11), and its associated radiation reaction force, Equations (4.16), (4.17)) make specific predictions, both for the motion and the radiation of BBHs. The analytical calculations underlying such an EOB description are essentially based on skeletonizing the two black holes as two, sufficiently separated point masses, and therefore seem unable to describe the merger of the two black holes, and the subsequent ringdown of the final, single black hole formed during the merger. However, as early as 2000 [40], the EOB formalism went one step further and proposed a specific strategy for describing the *complete* waveform emitted during the entire coalescence process, covering inspiral, merger, and ringdown. This EOB proposal is somewhat crude. However, the predictions it has made (years before NR simulations could accurately describe the late inspiral and merger of BBHs) have been broadly confirmed by subsequent NR simulations. (See Section 1 for a list of EOB predictions.) Essentially, the EOB proposal (which was motivated partly by the closeness between the 2PN-accurate effective metric $g^{\text{eff}}_{\mu\nu}$ [39] and the Schwarzschild metric, and by the results of Refs. [67] and [68]) consists of:

(i) defining, within EOB theory, the instant of (effective) "*merger*" of the two black holes as the (dynamical) EOB time t_m where the orbital frequency $\Omega(t)$ reaches its *maximum*;

(ii) describing (for $t \le t_m$) the inspiral-plus-plunge (or simply *insplunge*) waveform, $h^{\text{insplunge}}(t)$, by using the inspiral EOB dynamics and waveform reviewed in the previous section; and

(iii) describing (for $t \ge t_m$) the merger-plus-ringdown waveform as a superposition of several quasi-normal-mode (QNM) complex frequencies of a final Kerr black hole (of mass M_f and spin parameter a_f, self-consistency estimated within the EOB formalism), say

$$\left(\frac{Rc^2}{GM}\right) h^{\text{ringdown}}_{\ell m}(t) = \sum_N C^+_N \, e^{-\sigma^+_N (t-t_m)} \,, \tag{5.1}$$

with $\sigma^+_N = \alpha_N + i\,\omega_N$, and where the label N refers to indices (ℓ, ℓ', m, n), with (ℓ, m) being the Schwarzschild-background multipolarity of the considered (metric) waveform $h_{\ell m}$, with $n = 0, 1, 2\dots$, being the "overtone number" of the considered Kerr-background Quasi-Normal-Mode, and ℓ' the degree of its associated spheroidal harmonics $S_{\ell' m}(a\sigma, \theta)$;

(iv) determining the excitation coefficients C^+_N of the QNM's in Equation (5.1) by using a simplified representation of the transition between plunge and ring-down obtained by smoothly *matching* (following Ref. [78]), on a $(2p+1)$-toothed "comb" $(t_m - p\delta, \dots, t_m - \delta, t_m, t_m + \delta, \dots, t_m + p\delta)$ centered around the merger (and matching) time t_m, the inspiral-plus-plunge waveform to the above ring-down waveform.

Finally, one defines a complete, quasi-analytical EOB waveform (covering the full process from inspiral to ring-down) as

$$h_{\ell m}^{\rm EOB}(t) = \theta(t_m - t)\, h_{\ell m}^{\rm insplunge}(t) + \theta(t - t_m)\, h_{\ell m}^{\rm ringdown}(t)\,, \tag{5.2}$$

where $\theta(t)$ denotes Heaviside's step function. The final result is a waveform that essentially depends only on the choice of a resummed EOB $A(u)$ potential, and, less importantly, on the choice of resummation of the main waveform amplitude factor $f_{22} = (\rho_{22})^2$.

We have emphasized here that the EOB formalism is able, in principle, starting only from the best currently known analytical information, to predict the full waveform emitted by coalescing BBHs. The early comparisons between 3PN-accurate EOB predicted waveforms[7] and NR-computed waveforms showed a satisfactory agreement between the two, within the (then relatively large) NR uncertainties [97, 98]. Moreover, as we shall discuss below, it has been recently shown that the currently known Padé-resummed 3PN-accurate $A(u)$ potential is able, as is, to describe with remarkable accuracy several aspects of the dynamics of coalescing BBHs [99, 100].

On the other hand, when NR started delivering high-accuracy waveforms, it became clear that the 3PN-level analytical knowledge incorporated in EOB theory was not accurate enough for providing waveforms agreeing with NR ones within the high-accuracy needed for detection, and data analysis of upcoming GW signals. (See, e.g. the discussion in Section II of Ref. [91].) At that point, one made use of the *natural flexibility* of the EOB formalism. Indeed, as already emphasized in early EOB work [42, 101], we know from the analytical point of view that there are (yet uncalculated) further terms in the u-expansions of the EOB potentials $A(u), D(u), \dots$ (and in the x-expansion of the waveform), so that these terms can be introduced either as "free parameter(s) in constructing a bank of templates, and (one should) wait until" GW observations determine their value(s) [42], or as "*fitting parameters* and adjusted so as to reproduce other information one has about the exact results" (to quote Ref. [101]). For instance, modulo logarithmic corrections that will be further discussed below, the Taylor expansion in powers of u of the main EOB potential $A(u)$ reads

$$A^{\rm Taylor}(u;\nu) = 1 - 2u + \tilde{a}_3(\nu)u^3 + \tilde{a}_4(\nu)u^4 + \tilde{a}_5(\nu)u^5 + \tilde{a}_6(\nu)u^6 + \cdots\,,$$

where the 2PN and 3PN coefficients $\tilde{a}_3(\nu) = 2\nu$ and $\tilde{a}_4(\nu) = a_4\nu$ have been known since 2001, but where the 4PN, 5PN, ... coefficients, $\tilde{a}_5(\nu), \tilde{a}_6(\nu), \dots$ were not known

7 The new, resummed EOB waveform discussed above was not available at the time, so that these comparisons employed the coarser "Newtonian-level" EOB waveform $h_{22}^{(N,\epsilon)}(x)$.

at the time (see below for the recent determination of $\tilde{a}_5(\nu)$). A first attempt was made in [101] to use numerical data (on circular orbits of corotating black holes) to fit for the value of a (single, effective) 4PN parameter of the simple form $\tilde{a}_5(\nu) = a_5 \nu$ entering a Padé-resummed 4PN-level A potential, i.e.

$$A_4^1(u; a_5, \nu) = P_4^1 \left[A_{3\mathrm{PN}}(u) + \nu a_5 u^5 \right] . \tag{5.3}$$

This strategy was pursued in Refs. [79, 102] and many subsequent works. It was pointed out in Ref. [66] that the introduction of a further 5PN coefficient $\tilde{a}_6(\nu) = a_6 \nu$, entering a Padé-resummed 5PN-level A potential, i.e.

$$A_5^1(u; a_5, a_6, \nu) = P_5^1 \left[A_{3\mathrm{PN}}(u) + \nu a_5 u^5 + \nu a_6 u^6 \right] , \tag{5.4}$$

helped in having a closer agreement with accurate NR waveforms.

In addition, Refs. [78, 79] introduced another type of flexibility parameters of the EOB formalism: the non-quasi-circular (NQC) parameters accounting for uncalculated modifications of the quasi-circular inspiral waveform presented above, linked to deviations from an adiabatic quasi-circular motion. These NQC parameters are of various types, and subsequent works [66, 91, 93, 94, 103, 104] have explored several ways of introducing them. They enter the EOB waveform in two separate ways. First, through an explicit, additional complex factor multiplying $h_{\ell m}$, e.g.

$$f_{\ell m}^{\mathrm{NQC}} = (1 + a_1^{\ell m} n_1 + a_2^{\ell m} n_2) \exp[i(a_3^{\ell m} n_3 + a_4^{\ell m} n_4)] ,$$

where the n_i's are dynamical functions that vanish in the quasi-circular limit (with n_1, n_2 being time-even, and n_3, n_4 time-odd). For instance, one usually takes $n_1 = (p_{r_*}/r\Omega)^2$. Second, through the (discrete) choice of the argument used during the plunge to replace the variable x of the quasi-circular inspiral argument: e.g. either $x_\Omega \equiv (GM\Omega)^{2/3}$, or (following [106]) $x_\varphi \equiv v_\varphi^2 = (r_\omega \Omega)^2$ where $v_\varphi \equiv \Omega\, r_\omega$, and $r_\omega \equiv r[\psi(r, p_\varphi)]^{1/3}$ is a modified EOB radius, with ψ being defined as

$$\psi(r, p_\varphi) = \frac{2}{r^2} \left(\frac{dA(r)}{dr} \right)^{-1} \left[1 + 2\nu \left(\sqrt{A(r) \left(1 + \frac{p_\varphi^2}{r^2} \right)} - 1 \right) \right] . \tag{5.5}$$

For a given value of the symmetric mass ratio, and given values of the A-flexibility parameters $\tilde{a}_5(\nu), \tilde{a}_6(\nu)$ one can determine the values of the NQC parameters $a_i^{\ell m}$'s from accurate NR simulations of BBH coalescence (with mass ratio ν) by imposing, say, that the complex EOB waveform $h_{\ell m}^{\mathrm{EOB}}(t^{\mathrm{EOB}}; \tilde{a}_5, \tilde{a}_6; a_i^{\ell m})$ *osculates* the corresponding NR one $h_{\ell m}^{\mathrm{NR}}(t^{\mathrm{NR}})$ at their respective instants of "merger", where $t_{\mathrm{merger}}^{\mathrm{EOB}} \equiv t_m^{\mathrm{EOB}}$ was defined above (maximum of $\Omega^{\mathrm{EOB}}(t)$), while $t_{\mathrm{merger}}^{\mathrm{NR}}$ is defined as the (retarded) NR time where the modulus $|h_{22}^{\mathrm{NR}}(t)|$ of the quadrupolar waveform reaches its maximum. The order of osculation that one requires between $h_{\ell m}^{\mathrm{EOB}}(t)$ and $h_{\ell m}^{\mathrm{NR}}(t)$ (or, separately, between their moduli and their phases or frequencies) depends on the number of NQC parameters $a_i^{\ell m}$. For instance, $a_1^{\ell m}$ and $a_2^{\ell m}$ affect only the modulus of $h_{\ell m}^{\mathrm{EOB}}$ and allow one to match both $|h_{\ell m}^{\mathrm{EOB}}|$ and its first time derivative, at merger, to their NR counterparts, while $a_3^{\ell m}, a_4^{\ell m}$ affect only the phase of the EOB waveform, and allow one to match the GW frequency $\omega_{\ell m}^{\mathrm{EOB}}(t)$ and its first time derivative, at merger, to their NR counterparts. The above EOB/NR matching scheme has been developed and varied in various versions in Refs. [66, 76, 91, 93, 94, 103–105]. One has also extracted the needed matching data from accurate NR simulations, and provided explicit, analytical ν-dependent fitting formulas for them [66, 76, 91].

Having so "calibrated" the values of the NQC parameters by extracting nonperturbative information from a sample of NR simulations, one can then, for any choice of the A-flexibility parameters, compute a full EOB waveform (from early inspiral to late ringdown). The comparison of the latter EOB waveform to the results of NR simulations is discussed in the next section.

6 EOB vs NR

There have been several different types of comparison between EOB and NR. For instance, the early work [97] pioneered the comparison between a purely analytical EOB waveform (uncalibrated to any NR information) and a NR wavform, while the early work [107] compared the predictions for the final spin of a coalescing black hole binary made by EOB, *completed* by the knowledge of the energy and angular momentum lost during ringdown by an extreme mass ratio binary (computed by the test-mass NR code of [108]), to comparable-mass NR simulations [109]. Since then, many other EOB/NR comparisons have been performed, both in the comparable-mass case [66, 79, 93, 94, 98, 102, 103] and in the small-mass-ratio case [78, 104, 110, 111]. Note in this respect that the numerical simulations of the GW emission by extreme mass-ratio binaries have provided (and still provide) a very useful "laboratory" for learning about the motion and radiation of binary systems, and their description within the EOB formalism.

Here we shall discuss only two recent examples of EOB/NR comparisons, which illustrate different facets of this comparison.

6.1 EOB[NR] waveforms vs NR ones

We explained above how one could complete the EOB formalism by calibrating some of the natural EOB flexibility parameters against NR data. First, for any given mass ratio ν and any given values of the A-flexibility parameters $\tilde{a}_5(\nu), \tilde{a}_6(\nu)$, one can use NR data to uniquely determine the NQC flexibility parameters a_i's. In other words, we have (for a given ν)

$$a_i = a_i[\text{NR data}; a_5, a_6]\ ,$$

where we defined a_5 and a_6 so that $\tilde{a}_5(\nu) = a_5\nu, \tilde{a}_6(\nu) = a_6\nu$. (We allow for some residual ν-dependence in a_5 and a_6.) Inserting these values in the (analytical) EOB waveform then defines an NR-completed EOB waveform which still depends on the two unknown flexibility parameters a_5 and a_6.

In Ref. [66] the (a_5, a_6)-dependent predictions made by such a NR-completed EOB formalism were compared to the high-accuracy waveform from an equal-mass BBH ($\nu = 1/4$) computed by the Caltech–Cornell–CITA group [112], (and then made available on the web). It was found that there is a strong degeneracy between a_5 and a_6 in the sense that there is an excellent EOB-NR agreement for an extended region in the (a_5, a_6)-plane. More precisely, the phase difference between the EOB (metric) waveform and the Caltech–Cornell–CITA one, considered between GW frequencies $M\omega_L = 0.047$ and $M\omega_R = 0.31$ (i.e. the last 16 GW cycles before merger), stays smaller than 0.02 radians within a long and thin banana-like region in the (a_5, a_6)-plane. This "good region" approximately extends between the points $(a_5, a_6) = (0, -20)$ and $(a_5, a_6) = (-36, +520)$. As an example (which actually lies on the boundary of the "good region"), we shall consider here (following Ref. [113]) the specific values $a_5 = 0, a_6 = -20$ (to which correspond, when $\nu = 1/4$, $a_1 = -0.036347, a_2 = 1.2468$). (Ref. [66] did not make use of the NQC phase flexibility; i.e. it took $a_3 = a_4 = 0$. In addition, it introduced a (real) modulus NQC factor $f_{\ell m}^{\text{NQC}}$ only for the dominant quadrupolar wave $\ell = 2 = m$.) We henceforth use M as time unit. This result relies on the proper comparison between NR and EOB time series, which is a delicate subject. In fact, to compare the NR and EOB phase time-series $\phi_{22}^{\text{NR}}(t_{\text{NR}})$ and $\phi_{22}^{\text{EOB}}(t_{\text{EOB}})$ one needs to shift, by additive constants, both one of the time variables, and one of the phases. In other words, we need to determine τ and α such that the "shifted" EOB quantities

$$t'_{\text{EOB}} = t_{\text{EOB}} + \tau \qquad \phi_{22}^{\prime\text{EOB}} = \phi_{22}^{\text{EOB}} + \alpha \tag{6.1}$$

"best fit" the NR ones. One convenient way to do so is first to "pinch" (i.e. constrain to vanish) the EOB/NR phase difference at two different instants (corresponding to two different frequencies ω_1 and ω_2). Having so related the EOB time and phase variables to the NR ones we can straigthforwardly compare the EOB time series to its NR correspondant. In particular, we can compute the (shifted) EOB–NR phase difference

$$\Delta^{\omega_1,\omega_2}\phi_{22}^{\text{EOBNR}}(t_{\text{NR}}) \equiv \phi_{22}^{\prime\text{EOB}}(t'EOB) - \phi_{22}^{\text{NR}}(t^{\text{NR}}). \tag{6.2}$$

Figure 2 compares[8] (the real part of) the analytical EOB *metric* quadrupolar waveform $\Psi_{22}^{\text{EOB}}/\nu$ to the corresponding (Caltech–Cornell–CITA) NR *metric* waveform $\Psi_{22}^{\text{NR}}/\nu$. (Here, Ψ_{22} denotes the Zerilli-normalized asymptotic quadrupolar waveform, i.e.

8 The two "pinching" frequencies used for this comparison are $M\omega_1 = 0.047$ and $M\omega_2 = 0.31$.